

Seebeck effect in the graphene-superconductor junction

Marcin M. Wysocki^{1,*} and Jozef Spalek^{1,2,†}

¹*Marian Smoluchowski Institute of Physics, Jagiellonian University, Reymonta 4, PL-30-059 Kraków, Poland*

²*Faculty of Physics and Applied Computer Science,*

AGH University of Science and Technology, Reymonta 19, PL-30-059 Kraków, Poland

(Dated: May 2, 2019)

Thermopower of graphene-superconductor (GS) junction is analyzed within the extended Blonder-Tinkham-Klapwijk formalism. Within this approach we have also calculated the temperature dependence of the zero-bias conductance for GS junction. Both quantities reflect quasi-relativistic nature of massless Dirac fermions in graphene. Both, the linear and the non-linear regimes are considered.

PACS numbers: 74.45.+c, 73.23.Ad, 65.80.Ck

I. INTRODUCTION

Graphene is one of the most remarkable new materials. Not only has its discovery¹ violated in same sense Landau's theory of the thermodynamical instability of a two-dimensional structure², but also due to the peculiar band structure it has provided us with an invaluable opportunity to test relativistic quantum electrodynamics in the desktop laboratory³. For that reason, much effort has been put into understanding of the phenomena associated with this material.

Since the graphene-based devices are usually considered as a mesoscopic systems, the Landauer approach is widely utilized to study the ballistic transport in them⁴⁻⁶. Even though this approach does not account in the simplest form for all the features of the material, it provides a good overall description of the electric transport. This approach was extended by Blonder, Tinkham, and Klapwijk⁷ (BTK) to the case of standard normal metal-superconductor junction (NS), and in this manner yielded a very good description of experimental data⁸. Their method has been widely used for different specific situations⁹⁻¹⁷ and finally adapted for graphene-superconductor hybrid systems¹⁸⁻²². One of the most peculiar properties predicted in such systems is the specular Andreev reflection and deviations of the conductance spectra¹⁸ from those predicted by BTK for normal metals⁷.

Landauer formalism has also been successfully adapted for thermoelectrical transport in mesoscopic devices²³⁻²⁵. In the case of standard NS junctions BTK formula, also turned out to be useful technique for predicting effects concerning thermal properties of electric and heat currents^{11,13,17,26}. This method has also been used for the graphene-based superconducting hybrid structures for obtaining the thermal conductance^{20,27-29}. However, the thermopower has not been studied so far. This topic is addressed in this article.

In this work we provide systematic study of the effect of the temperature on the charge current in the superconducting graphene junction (GS) using a generalized BTK formalism for the specific case of graphene. We

present results concerning the temperature dependence of the zero-bias conductance and the Seebeck coefficient in the linear regime. For the sake of completeness, we also discuss the non-linear thermopower.

The paper is organized as follows. In Sec. II (and in Appendix A), we present briefly a generalized BTK approach for the charge current through the GS junction. The linear transport coefficients are discussed, in particular the zero-bias conductance and the thermopower. We also briefly comment on the effect of non-linear corrections on the Seebeck coefficient. Finally, we conclude in the Sec. IV.

II. MODEL

We consider a ballistic limit for graphene based junction composed of the normal region and induced by means of the proximity effect superconducting region (cf. Fig.1). For the description of the unconventional quasiparticle states we utilize Dirac - Bogoliubov - de Gennes equations for the two-dimensional (2D) sheet of graphene in the form^{18,30}

$$\begin{pmatrix} H_j - E_F \mathbf{1} & \Delta \\ \Delta^\dagger & E_F \mathbf{1} - H_j \end{pmatrix} \begin{pmatrix} u \\ v \end{pmatrix} = \epsilon \begin{pmatrix} u \\ v \end{pmatrix}, \quad (1)$$

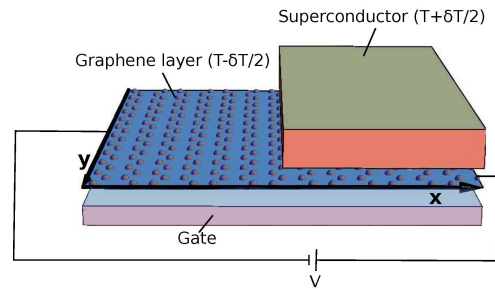


FIG. 1: (Color online) Proposed schematic, experimental setup considered in our modeling.

where the index j can be either + or - what refers to the two inequivalent valleys K and K' in the Brillouin zone. The single particle Hamiltonian is given by

$$H_{\pm} = -i\hbar v_F(\sigma_x \partial_x \pm \sigma_y \partial_y) + U, \quad (2)$$

where v_F is the energy independent Fermi velocity for the graphene, and $\{\sigma_i\}$ denote respective Pauli matrices. Because of the valley degeneracy one can effectively do the calculation for the one valley only. We assume that in the geometry, where the interface is determined by the y -axis, the pair potential with the s -wave symmetry changes step-like in the x -axis direction,

$$\Delta(\mathbf{r}, T) = \begin{cases} 0 & x < 0, \\ \Delta(T)e^{i\phi} & x > 0, \end{cases} \quad (3)$$

where the temperature dependence of the gap function can be deduced from the usual BCS theory³¹ and is taken in the following form

$$\frac{\Delta(T)}{\Delta_0} = \tanh \left(\sqrt{1.76 \cdot \sqrt{\frac{T_c}{T}} - 1} \right). \quad (4)$$

The BCS theory of the superconductivity based on the requirement that the coherence length is large when compared to the Fermi wavelength. Under that condition we can assume that the additional potential U has the form,

$$U(\mathbf{r}) = \begin{cases} 0 & x < 0, \\ -U_0 & x > 0, \end{cases} \quad (5)$$

with large U_0 ($E_F + U_0 \gg \Delta_0$) and for the simplicity we define $E'_F = E_F + U_0$. In numerical calculations we set $E'_F = 1000\Delta_0$.

In the spirit of the BTK scheme (by matching the wave functions at the boundary ($x = 0$)), we obtain expressions for the amplitudes of the Andreev hole reflection (AR) ($a(\epsilon, \theta)$) and the normal reflection ($b(\epsilon, \theta)$) of the incident electron - see Appendix A for details of the method. Note that there is no intrinsic barrier at the GS junction, and thus the Fermi vector mismatch is the source of the normal reflection. The transmission probability, averaged over the angles, takes the following form^{7,14},

$$\mathcal{T}(\epsilon) = \int_{-\pi/2}^{\pi/2} d\theta \frac{\cos \theta}{2} \left(1 - |b(\epsilon, \theta)|^2 + \frac{\text{Re}[e^{i\theta A}]}{\cos \theta} |a(\epsilon, \theta)|^2 \right). \quad (6)$$

The BTK formalism combined with the specific transmission probability derived for graphene, defines charge current through the GS interface as^{7,18},

$$I_e = \frac{4e}{h} \int_{-\infty}^{\infty} d\epsilon N(\epsilon) \mathcal{T}(\epsilon) (f^G(\epsilon - eV) - f^S(\epsilon)), \quad (7)$$

where f^G , f^S are the Fermi distribution functions for the normal (G) and the superconducting (S) region of GS junction respectively, and

$$N(\epsilon) = \frac{|E_F + \epsilon|W}{\pi \hbar v_F}, \quad (8)$$

is the energy dependent number of transverse modes in the graphene sheet of width W ¹⁸. However, formula (7) is not always accurate. The additional assumption is needed, that for each mode carrying incident electron, having energy $E_F + \epsilon$ and being Andreev reflected there is always enough modes at the level $E_F - \epsilon$ for this process to happen. However, away from perfect Andreev reflection regime ($|a(\epsilon)|^2 \neq 1$), as in our case, formula (7) remains rigorous.

The quantity describing thermoelectric properties of the system is thermopower, or Seebeck coefficient (S) measuring the voltage driving to zero the current flowing in response to the temperature difference, namely

$$S \equiv - \left(\frac{V}{\delta T} \right)_{I_e=0}. \quad (9)$$

III. CHARGE TRANSPORT

A. Linear regime

Expansion of the Fermi functions in the normal and superconducting regions to the first (linear) order in both the bias and the temperature difference, with the average temperature T , i.e.,

$$\begin{aligned} f^G &\equiv f_{T-\delta T/2}(\epsilon - eV) \simeq f_T(\epsilon) - eV \frac{\partial f}{\partial \epsilon} + \frac{\delta T}{2T} \epsilon \frac{\partial f}{\partial \epsilon}, \\ f^S &\equiv f_{T+\delta T/2}(\epsilon) \simeq f_T(\epsilon) - \frac{\delta T}{2T} \epsilon \frac{\partial f}{\partial \epsilon}, \end{aligned} \quad (10)$$

enables to decouple Eq.(7) in the form,

$$I_e = GV + I_e^T \delta T. \quad (11)$$

The resulting from it the linear transport coefficients can be thus rewritten in the following closed forms,

$$\begin{aligned} G &= -\frac{4e^2}{h} \int_{-\infty}^{\infty} d\epsilon \frac{\partial f}{\partial \epsilon} N(\epsilon) \mathcal{T}(\epsilon), \\ I_e^T &= \frac{4e}{hT} \int_{-\infty}^{\infty} d\epsilon \frac{\partial f}{\partial \epsilon} \epsilon N(\epsilon) \mathcal{T}(\epsilon). \end{aligned} \quad (12)$$

The temperature gradient and the bias are set as positive with respect to x coordinate. For the temperature in the system approaching zero, the expression for the electric conductance (G) reduces to the well-known BTK zero-bias conductance formula⁷

$$G_{T \rightarrow 0} = \frac{4e^2}{h} N(0) \mathcal{T}(0). \quad (13)$$

In Fig.2 we have plotted the zero-bias differential conductance (calculated from Eq.(12)) as a function of temperature, normalized by the ballistic conductance g_0 with having N transverse modes in a sheet of graphene of width W and given by

$$g_0 = \frac{4e^2}{h} \int_{-\infty}^{\infty} d\epsilon \frac{\partial f}{\partial \epsilon} N(\epsilon). \quad (14)$$

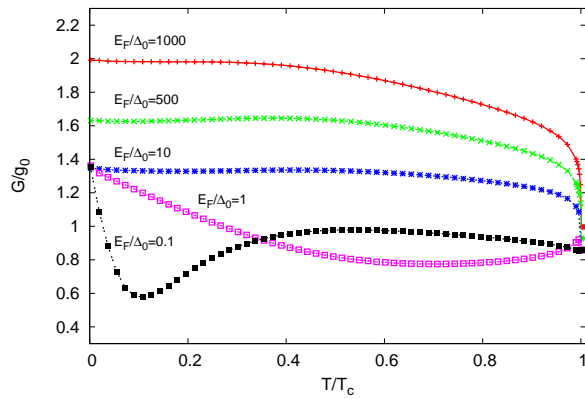


FIG. 2: (Color online) Normalized zero-bias conductance as a function of temperature for various Fermi vector mismatch.

For relatively high position of the Fermi level in graphene (roughly $E_F \gtrsim 5\Delta_0$), the influence of the increasing temperature (up to the approximately $T/T_c = 0.5$) on the conductance is almost negligible (cf. Fig. 2). The origin of this behavior is strictly connected with the relatively slow variation of the transmission probability $\mathcal{T}(\epsilon)$ for the subgap energies in this temperature regime, and thus does not differ qualitatively from the standard NS case⁷. In the low doping regime ($E_F \lesssim 5\Delta_0$), the linear differential conductance as a function of the temperature vastly differs from the standard NS case and reflects the specific electronic nature of graphene, as well as the impact of a crossover from the retro to the specular AR limit.

The non-trivial behavior of the Dirac fermions in graphene has also its influence on the linear thermopower. From Eq. (9) and (11) formula for this quantity reads

$$S = \frac{I_e^T}{G} = -\frac{1}{k_B T} \frac{\int_{-\infty}^{\infty} d\epsilon \epsilon |\epsilon + E_F| \frac{\partial \mathcal{I}}{\partial \epsilon} \mathcal{T}(\epsilon)}{\int_{-\infty}^{\infty} d\epsilon |\epsilon + E_F| \frac{\partial \mathcal{I}}{\partial \epsilon} \mathcal{T}(\epsilon)} \frac{k_B}{e}. \quad (15)$$

Results obtained by the numerical integration are presented in the Fig. 3. The low temperature regime differs from the one obtained for the NS junction¹¹. Contrary to the NS case, for the graphene-based structure the thermopower does not vanish for non-zero temperatures. This is due to the relativistic nature of charge carriers in graphene, where AR does not vanish even for the high effective barrier in our case (effective barrier is only due to the Fermi level mismatch) for the subgap energies (for the normal incidence AR happens always with certainty¹⁸). Furthermore, in the low doping regime ($E_F \lesssim \Delta_0$) the Seebeck coefficient for the GS junction is around one order of magnitude larger than even for high effective barrier value (which as a phenomenological parameter, can incorporate also the Fermi velocity mismatch⁸) in the NS case¹¹.

In this regime, we observe a clear maximum in the temperature dependence of the Seebeck coefficient in the su-

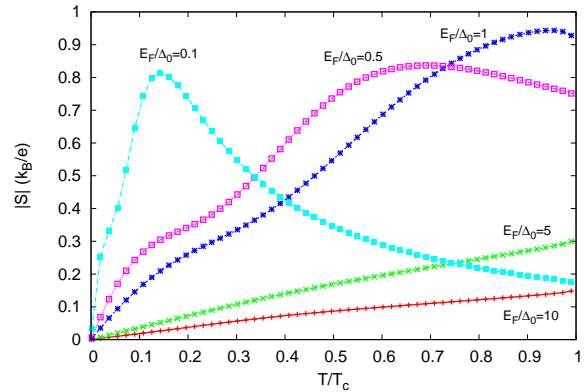


FIG. 3: (Color online) Linear thermopower as a function of temperature in the system for various Fermi vector mismatch.

perconducting state. The maximum roughly corresponds to the minimum in the zero-bias conductance as a function of temperature (cf. Fig. 2). The source of the significant enhancement of the thermopower in the low doping regime ($E_F \lesssim \Delta_0$) should be understood as an effect of being partly in the specular AR limit, where the transmission probability spectrum drops to zero for energy corresponding to the Fermi level position¹⁸. This feature affects the zero-bias conductance as a function of temperature and in turns is responsible for the thermopower increase in the specular AR limit. Therefore in this regime, the thermopower is large and reaches values up to $1k_B/e$. This suggests that there is a potential for application of this setup for cooling of various nanostructures.

B. Effect of the non-linearity

We have also studied numerically the effect of the non-linearity in our system. The thermopower in the non-linear regime can be calculated as a ratio between the bias voltage and the temperature gradient, when no charge current is flowing (c.f. Eq.(9)). The results in the non-linear regime are presented in Fig. 4. We have found that the non-linearity influences the thermopower in a not systematical manner with changing Fermi level position and the average temperature of the system. However the change is not as dramatic as in the NS case¹¹ and is almost unnoticeable in the doped regime $E_F \gtrsim 5\Delta_0$.

IV. CONCLUSIONS

In this work we have analyzed the thermoelectric charge transport in the graphene junction consisting of the normal and the superconducting parts. In the linear regime we have calculated the temperature dependence of the zero-bias conductance and the thermopower. We

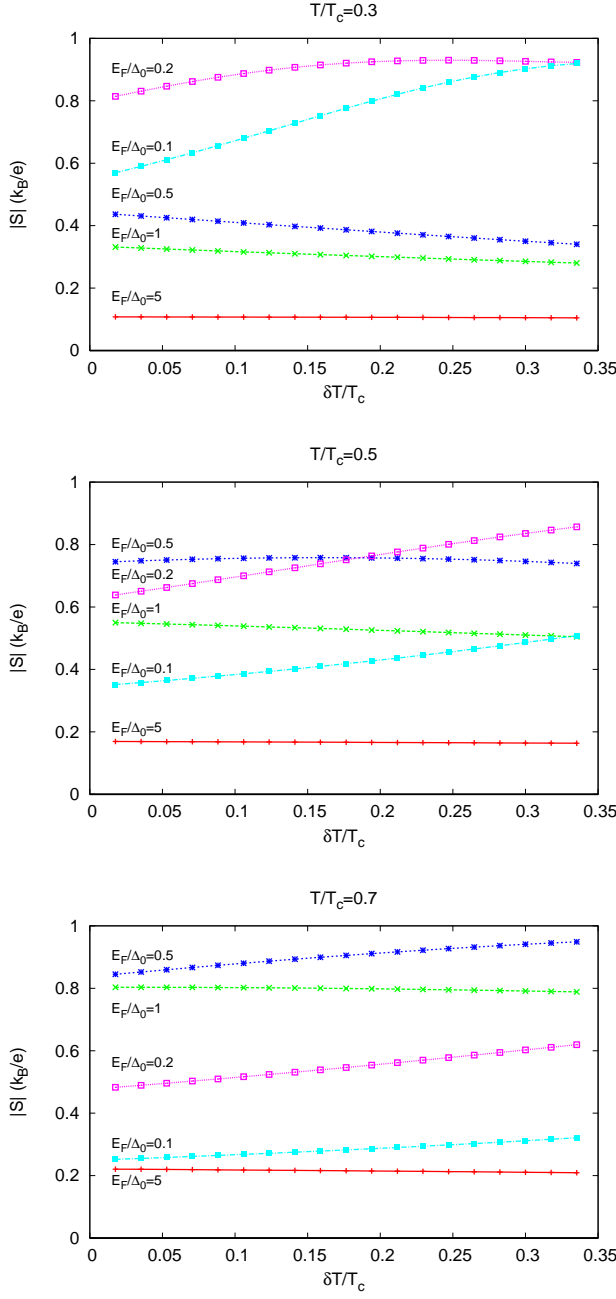


FIG. 4: (Color online) Nonlinear thermopower as a function of the temperature gradient set over the junction for various Fermi energies in graphene. The net temperature in the system is marked above each plot.

have found deviations of these quantities from the standard normal metal-superconductor junction case that are caused by the relativistic nature of electrons in graphene. In the specular Andreev reflection regime Seebeck coefficient is strongly enhanced for specific temperatures.

We have also studied the effect of non-linearity on the thermopower and we have found that for a high Fermi level positions ($E_F \gtrsim \Delta_0$) it stays almost unaffected and in the low Fermi level regime is noticeably enhanced with the increase of the temperature gradient.

Acknowledgements:

The authors greatly appreciate the stimulated discussion with Adam Rycerz, Jan Kaczmarczyk and Marcin Abram. The work has been partially supported by the Foundation for Polish Science (FNP) under the TEAM program. We also acknowledge the Grant MAESTRO from the National Science Center (NCN).

Appendix A: BTK for graphene

The wave function in the normal part of graphene (NG) ψ_N and in the superconducting region (SG) ψ_S , look respectively as follows

$$\begin{aligned} \psi_N &= \psi_N^{e+} + b\psi_N^{e-} + a\psi_N^{h-} \\ \psi_S &= c\psi_S^{e+} + d\psi_S^{h+}, \end{aligned} \quad (\text{A1})$$

where the superscripts e, h refers to electron and hole in NG and electronlike and holelike excitation in SG, and the superscripts $+$ and $-$ to right and left moving particle respectively.

Spinors resulting from Eq.(1) are expressed in the similar manner as in the Ref. 19, i.e., in the form

$$\begin{aligned} \psi_N^{e\pm} &= [1, \pm e^{\pm i\theta}, 0, 0]^T e^{\pm i k^e x \cos \theta}, \\ \psi_N^{h-} &= [0, 0, 1, e^{-i\theta_A}]^T e^{-i k^h x \cos \theta_A}, \\ \psi_S^{e+} &= [u, u e^{i\theta_S^e}, v e^{-i\phi}, v e^{i(\theta_S^e - \phi)}]^T e^{i q^e x \cos \theta_S^e}, \\ \psi_S^{h-} &= [v, -v e^{-i\theta_S^h}, u e^{-i\phi}, -u e^{-i(\theta_S^h + \phi)}]^T e^{-i q^h x \cos \theta_S^h}, \end{aligned} \quad (\text{A2})$$

where for the sake of clarity we do not include phase factor $e^{i k_y y}$ since it corresponds to conservation of momentum in \hat{y} direction. The corresponding wave vectors are defined as follows,

$$k^{e(h)} = \frac{\epsilon + (-)E_F}{\hbar v_F}, \quad q^{e(h)} = \frac{E'_F + (-)\sqrt{\epsilon^2 - \Delta^2}}{\hbar v_F}, \quad (\text{A3})$$

and the coherence factors are given by

$$u = \sqrt{\frac{1}{2} \left(1 + \frac{\sqrt{\epsilon^2 - \Delta^2}}{\epsilon} \right)}, \quad v = \sqrt{\frac{1}{2} \left(1 - \frac{\sqrt{\epsilon^2 - \Delta^2}}{\epsilon} \right)}. \quad (\text{A4})$$

The conservation of momentum at the interface and along \hat{y} direction enables us to obtain mutual relations for the specific angles, namely

$$k^e \sin \theta = k^h \sin \theta_A = q^e \sin \theta_S^e = q^h \sin \theta_S^h. \quad (\text{A5})$$

The system must also satisfy the continuity condition at the interface, $\psi_{\sigma L}(0) = \psi_{\sigma R}(0)$. The Hamiltonian is linear therefore is no need in matching derivatives. The resulting wave function amplitudes take the form,

$$\begin{aligned}
a(\epsilon, \theta) &= \frac{2 \cos \theta (e^{-i\theta_S^h} + e^{i\theta_S^c})uv}{(e^{-i\theta_A} + e^{-i\theta_S^h})(e^{-i\theta} + e^{i\theta_S^c})u^2 - (e^{-i\theta} - e^{-i\theta_S^h})(e^{-i\theta_A} - e^{i\theta_S^c})v^2}, \\
b(\epsilon, \theta) &= \frac{2 \cos \theta [(e^{i\theta_S^c} - e^{-i\theta_A})v^2 + (e^{-i\theta_S^h} + e^{-i\theta_A})u^2]}{(e^{-i\theta_A} + e^{-i\theta_S^h})(e^{-i\theta} + e^{i\theta_S^c})u^2 - (e^{-i\theta} - e^{-i\theta_S^h})(e^{-i\theta_A} - e^{i\theta_S^c})v^2} - 1.
\end{aligned} \tag{A6}$$

-
- * Electronic address: marcin.wysokinski@uj.edu.pl
† Electronic address: ufspalek@if.uj.edu.pl
- ¹ K. S. Novoselov, A. K. Geim, S. V. Morozov, D. Jiang, M. I. Katsnelson, I. V. Grigorieva, S. V. Dubonos, and A. A. Firsov, *Nature* **438**, 197 (2005).
 - ² L. D. Landau and J. M. Lifshitz *Statistical Physics* (Pergamon, Oxford, 1980).
 - ³ C. W. J. Beenakker, *Rev. Mod. Phys.* **80**, 1337 (2008).
 - ⁴ J. Tworzydło, B. Trauzettel, M. Titov, A. Rycerz, and C. W. J. Beenakker, *Phys. Rev. Lett.* **96**, 246802 (2006).
 - ⁵ I. Snyman and C. W. J. Beenakker, *Phys. Rev. B* **75**, 045322 (2007).
 - ⁶ Y. Xing, Q. Sun, and J. Wang, *Phys. Rev. B* **80**, 235411 (2009).
 - ⁷ G. E. Blonder, M. Tinkham, and T. M. Klapwijk, *Phys. Rev. B* **25**, 4515 (1982).
 - ⁸ G. E. Blonder and M. Tinkham, *Phys. Rev. B* **27**, 112 (1983).
 - ⁹ J. Kaczmarczyk, M. Sadzikowski, and J. Spalek, *Phys. Rev. B* **84**, 094525 (2011).
 - ¹⁰ J. Kaczmarczyk, M. Sadzikowski, and J. Spalek, *Physica C* **471**, 193 (2011).
 - ¹¹ M. Wysokiński, *Acta Phys. Pol. A* **122**, 758 (2012).
 - ¹² G. Annunziata, H. Enoksen, J. Linder, M. Cuoco, C. Noce, and A. Sudbø, *Phys. Rev. B* **83**, 144520 (2011).
 - ¹³ A. Bardas and D. Averin, *Phys. Rev. B* **52**, 12873 (1995).
 - ¹⁴ N. A. Mortensen, K. Flensberg, and A. P. Jauho, *Phys. Rev. B* **59**, 10176 (1999).
 - ¹⁵ Y. Tanaka and S. Kashiwaya, *Phys. Rev. Lett.* **74**, 3451 (1995).
 - ¹⁶ V. Lukic and E. J. Nicol, *Phys. Rev. B* **76**, 144508 (2007).
 - ¹⁷ J. E. Hirsch, *Phys. Rev. B* **50**, 3165 (1994).
 - ¹⁸ C. W. J. Beenakker, *Phys. Rev. Lett.* **97**, 067007 (2006).
 - ¹⁹ J. Linder and A. Sudbø, *Phys. Rev. B* **77**, 064507 (2008).
 - ²⁰ T. Yokoyama, J. Linder, and A. Sudbø, *Phys. Rev. B* **77**, 132503 (2008).
 - ²¹ Q. Zhang, D. Fu, B. Wang, R. Zhang, and D. Y. Xing, *Phys. Rev. Lett.* **101**, 047005 (2008).
 - ²² M. Titov and C. W. J. Beenakker, *Phys. Rev. B* **74**, 041401 (2006).
 - ²³ U. Sivan and Y. Imry, *Phys. Rev. B* **33**, 551 (1986).
 - ²⁴ P. N. Butcher, *J. Phys.: Condens Matter* **2**, 4869 (1990).
 - ²⁵ H. van Houten, L. W. Molenkamp, C. W. J. Beenakker, and C. T. Foxon, *Semicond. Sci. Technol.* **7**, B215 (1992).
 - ²⁶ I. A. Devyatov and M. Yu Romashka and A. V. Burmistrova, *JETP Lett.* **91**, 297 (2010).
 - ²⁷ M. Titov, A. Ossipov, and C. W. J. Beenakker, *Phys. Rev. B* **75**, 045417 (2007).
 - ²⁸ M. Salehi, M. Alidoust, and G. Rashedi, *J. Appl. Phys.* **108**, 083917 (2010).
 - ²⁹ M. Salehi, M. Alidoust, Y. Rahnavard, and G. Rashedi, *J. Appl. Phys.* **107**, 123916 (2010).
 - ³⁰ P. G. de Gennes, *Superconductivity in Metals and Alloys* (W. A. Benjamin, New York, 1966).
 - ³¹ J. B. Ketterson and S. N. Song, *Superconductivity* (Cambridge University Press, 1999).